Power-law scaling in Bénard-Marangoni convection at large Prandtl numbers

Thomas Boeck
Max-Planck-Institute for the Physics of Complex Systems, Nöthnitzer Strasse 38, 01187 Dresden, Germany

André Thess
Department of Mechanical Engineering, Ilmenau University of Technology, P.O. Box 100565, 98684 Ilmenau, Germany

(Received 23 March 2001; published 18 July 2001)

Bénard-Marangoni convection at large Prandtl numbers is found to exhibit steady (nonturbulent) behavior in numerical experiments over a very wide range of Marangoni numbers Ma far away from the primary instability threshold. A phenomenological theory, taking into account the different character of thermal boundary layers at the bottom and at the free surface, is developed. It predicts a power-law scaling for the nondimensional velocity (Peclet number) and heat flux (Nusselt number) of the form $\mathrm{Pe}\sim\mathrm{Ma}^{2/3}$, $\mathrm{Nu}\sim\mathrm{Ma}^{2/9}$. This prediction is in good agreement with two-dimensional direct numerical simulations up to $\mathrm{Ma}=3.2\times10^5$.

DOI: 10.1103/PhysRevE.64.027303 PACS number(s): 47.27.Te, 47.20.Dr, 47.15.Gf, 47.15.Cb

I. INTRODUCTION

Turbulent Rayleigh-Bénard convection [1] has been explored over a wide range of Rayleigh numbers Ra and Prandtl numbers P, thanks to the comprehensive joint effort of experimental [2–6], analytical [7,8], and two-dimensional [9] and three-dimensional [10] numerical studies. In particular, the development of experimental techniques for handling substances such as He or SF_6 in the vicinity of their critical points has permitted one to analyze convection at large Prandtl numbers [6] in great detail.

In contrast to buoyancy-driven Rayleigh-Bénard convection, the understanding of surface-tension-driven Bénard-Marangoni convection [11] is relatively poor. In spite of its widespread occurence in materials processing [12] and chemical engineering [13], phenomenological models predicting the scaling of the Nusselt number Nu on the Marangoni number Ma have only recently begun to appear [14]. The present paper focuses on such scaling behavior in Bénard-Marangoni convection in large-Prandtl-number fluids employing both two-dimensional numerical simulations and boundary layer analyses. In contrast to Rayleigh-Bénard convection, the simulations do not show a transition to time-dependent or turbulent flow even at Ma more than 4000 times the critical value. For such high values of Ma, the heat transport in the (laminar) simulations shows scaling on Ma. The exponent is in good agreement with the result $\mathrm{Nu}\sim\mathrm{Ma}^{2/9}$ derived from a boundary layer analysis of the temperature field.

II. MATHEMATICAL MODEL

We consider a one-layer approximation for two-dimensional Bénard-Marangoni convection [15]. The heat flux density q at the free surface is prescribed. The nondimensional computational model in the domain $0\leqslant z\leqslant 1$, with periodic boundary conditions in x, comprises the following dimensionless equations and boundary conditions:

$$P^{-1}[\partial_t\mathbf{v}+(\mathbf{v}\cdot\boldsymbol{\nabla})\mathbf{v}]=-\boldsymbol{\nabla}p+\boldsymbol{\nabla}^2\mathbf{v}, \tag{1a}$$

$$\boldsymbol{\nabla}\cdot\mathbf{v}=0, \tag{1b}$$

$$\partial_t T+(\mathbf{v}\cdot\boldsymbol{\nabla})T=\boldsymbol{\nabla}^2 T, \tag{1c}$$

$$v_x=v_z=0,\quad T=1\quad(\text{at } z=0), \tag{1d}$$

$$v_z=0,\quad \partial_z T=-1,\quad \partial_z v_x=-Ma\,\partial_x T\quad(\text{at } z=1). \tag{1e}$$

Equations (1) are based on the layer thickness d as the unit of length, d^2/κ as the unit of time, and qd/λ as the unit of temperature, where λ denotes the heat conductivity of the fluid. Velocity $\mathbf{v}=v_x\mathbf{e}_x+v_z\mathbf{e}_z$ and temperature T depend on x and z only. The Prandtl number $P=\nu/\kappa$ represents the ratio of kinematic viscosity and thermal diffusivity. The Marangoni number is defined as $\mathrm{Ma}=\gamma q d^2/\lambda\rho\nu\kappa$, where ρ denotes the density of the fluid and $\gamma=-d\sigma/dT$ is the (negative) derivative of the surface tension with respect to the temperature.

The instability of the basic state $\mathbf{v}=0$, $T=1-z$ occurs above $\mathrm{Ma}_c\approx 79.6$ for a wave number $k_c\approx 1.99$ [15]. Since the heat flux is prescribed, convection reduces the temperature difference across the layer. Therefore, the Nusselt number is defined as

$$\mathrm{Nu}=1/\Delta T, \tag{2}$$

where ΔT denotes the mean temperature difference between the bottom and the free surface.

We solve system (1) numerically using a streamfunction-vorticity based, pseudospectral Fourier-Chebyshev method. The scheme is similar to that presented in Ref. [16]. In order to ensure high resolution with a moderate number of modes, we consider a single basic cell of length $L=2\pi/k_c$.

The goal of the simulations was to determine the behavior of Bénard-Marangoni convection in the limit of large Peclet and small Reynolds numbers, i.e., in the case of strong forcing by the instability mechanism but with sufficiently large Prandtl numbers to render the convective terms in the Navier-Stokes equations negligible. Therefore, we have chosen to consider the limit of infinite Prandtl number. The neglect of nonlinear terms reduces the computational load in

TABLE I. Simulation parameters and data. N_x and N_z denote the number of collocation points. The quantity $\langle T\rangle(0)-\langle T\rangle(0.5)$ is an estimate of the thickness of the thermal boundary layer at the bottom.

Ma	N_x	N_z	u	Nu	$\langle T\rangle(0)-\langle T\rangle(0.5)$
1.0×10^4	512	65	5.46×10^1	3.98	0.222
2.0×10^4	512	65	8.74×10^1	4.71	0.188
4.0×10^4	1024	129	1.40×10^2	5.56	0.160
8.0×10^4	1024	129	2.24×10^2	6.56	0.137
1.6×10^5	1024	129	3.59×10^2	7.72	0.117
3.2×10^5	2048	129	5.75×10^2	9.08	0.100

the simulations considerably. The applicability of this limit for high-Prandtl-number Bénard-Marangoni convection was already demonstrated in a number of theoretical and numerical studies [17,18]. For our case, the computational results for infinite P and $P=100$, which is a typical value for silicone oils, match closely up to values of $\mathrm{Ma}\approx10^5$, i.e., for more than three decades above the onset of instability. Table I shows the simulation results and the numerical parameters used. With three-dimensional simulations, such high values of Ma are currently not accessible.

III. RESULTS

An unexpected observation in all our numerical simulations was the complete absence of time-dependent flows and the reproducible evolution toward robust stationary rolls (shown in Fig. 1) from arbitrary initial conditions. Although Ma exceeded Ma_c by more than three orders of magnitude, no temporal change was observed in the boundary layer structure of the temperature field [Figs 1(a) and 1(b)] and in the streamlines [Fig 1(c) and 1(d)]. In contrast, in Rayleigh-Bénard convection between free-slip boundaries, the flow becomes time-dependent at $\mathrm{Ra}\approx4\times10^4$ [19], which is about 10^2 times the critical value for onset of convection. Although our observations do not exclude the possibility of instability and time-dependent behavior at even larger Ma, this scenario does not seem very likely.

One heuristic argument supporting this view is based on the coupling between temperature and flow fields. In Rayleigh-Bénard convection, the buoyancy term couples the temperature and velocity distributions throughout the fluid. In Bénard-Marangoni convection, the equations for velocity and temperature decouple in the bulk. Only the Marangoni boundary condition at the free surface transmits information on the temperature distribution to the velocity field. This may be a severe limitation for the occurence of instabilities of the steady rolls. Moreover, the lateral temperature gradients at the free surface do not grow sufficiently fast to support the hydrothermal wave instability [20]. A final answer on this issue requires a linear stability analysis of the roll solutions.

The absence of secondary bifurcations simplifies the analysis of the asymptotic state. Figure 1 shows that, upon increasing the Marangoni number, thermal boundary layers form around an isothermal core in the center of the rolls. Vertical temperature profiles plotted in Fig. 2, which represent horizontal averages, are particularly striking. The streamline pattern in the bulk remains approximately the same. Strong velocity gradients occur only at the downflow regions of the free surface. The spatial rms velocity u (i.e., the Péclet number) is shown as function of Ma in Fig. 3(a). Our numerical results are very well fitted by

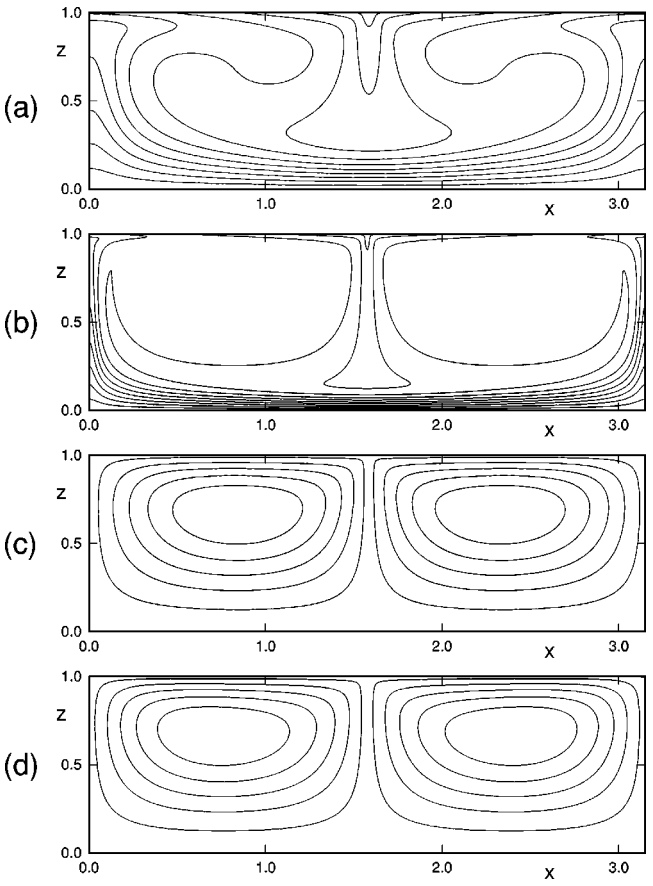

FIG. 1. Isotherms [(a) and (b)] and streamlines [(c) and (d)] for $P=\infty$ and $\mathrm{Ma}=10^4$ [(a) and (c)] and $\mathrm{Ma}=3.2\times10^5$ [(b) and (d)].

$$u\sim\mathrm{Ma}^{0.68}. \tag{3}$$

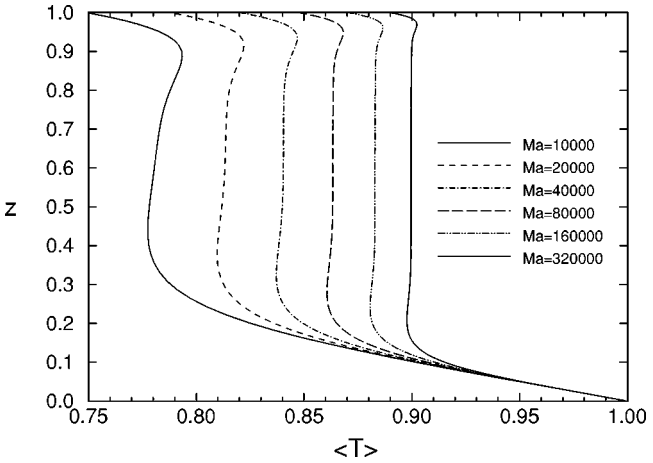

FIG. 2. Vertical profiles of the horizontally averaged temperature $\langle T\rangle$ for $P=\infty$.

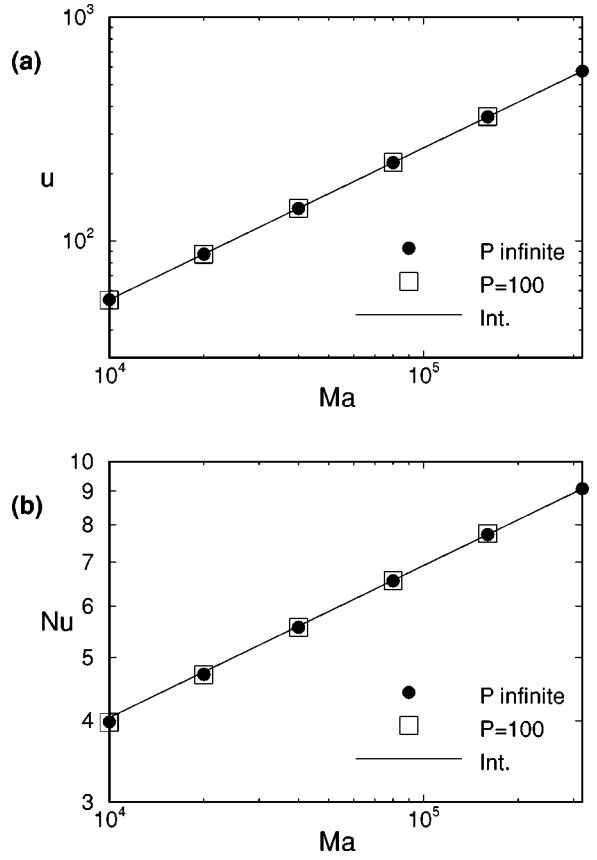

FIG. 3. Power-law scaling of (a) the rms velocity u (i.e., the Péclet number) and (b) the Nusselt number Nu on Ma. The straight lines (power laws) interpolate the values for $\mathrm{Ma}=1.6\times10^5$ and $\mathrm{Ma}=3.2\times10^5$ ($P=\infty$). Data for $P=100$ are very close to the values for infinite P.

For Nu as a function of Ma [Fig. 3(b)], a power-law fit is not as exact, but still rather good. We obtain

$$\mathrm{Nu}\sim\mathrm{Ma}^{0.24} \tag{4}$$

from our numerical data.

The observed scaling exponents can be explained by a simple phenomenological model. The derivation of the model is very similar to that presented in Ref. [16] for inertial Bénard-Marangoni convection. We shall not take the detailed flow structure such as corner regions of the rolls, into account. A more refined approach including these details could be guided by the models of Roberts [21] for two-dimensional Rayleigh-Bénard convection at infinite Prandtl number.

The cornerstone of the model is the kinetic-energy budget. For steady convection, energy input through the Marangoni effect is equal to dissipation through viscosity. For a single roll cell located in the interval $0\leqslant x\leqslant L/2$, we have the exact relation

$$-\mathrm{Ma}\int_0^{L/2} v_x\partial_x T dx=\int_0^1\int_0^{L/2}\omega^2 dxdz, \tag{5}$$

where $\omega=\partial_z v_x-\partial_x v_z$ denotes the vorticity. The integral on the left hand side is evaluated at the free surface $z=1$. We shall now estimate the terms in the energy budget. L is assumed to be of order unity, and is not taken into account any further. The right hand side is then just $\sim u^2$. On the left hand side we assume that the velocity at the free surface is $\sim u$. We then have to estimate the surface temperature difference across the roll. As for inertial convection [16], we assume that it is of the same order as the temperature drop ΔT_{top} across the free surface thermal boundary layer. Putting these estimates into Eq. (5) yields

$$\mathrm{Ma}\,\Delta T_{top}u\sim u^2. \tag{6}$$

In order to determine ΔT_{top}, we first estimate the thickness δ_{top} of the free surface boundary layer. The horizontal velocity is of order u throughout the free surface thermal boundary layer. From the boundary condition $\partial_z T=-1$ at $z=1$ and the estimate $\delta_{top}\sim u^{-1/2}$, it follows that

$$\Delta T_{top}\sim u^{-1/2}. \tag{7}$$

Using Eqs. (6) and (7), we obtain the scaling law

$$u\sim\mathrm{Ma}^{2/3}, \tag{8}$$

where the exponent is in excellent agreement with the numerical value of 0.68 in Eq. (3).

For the Nusselt number defined in Eq. (2), the total temperature difference

$$\Delta T=\Delta T_{top}+\Delta T_{bot} \tag{9}$$

must be estimated, where ΔT_{bot} denotes the temperature difference across the bottom boundary layer. In contrast to the free surface, v_x is zero at $z=0$. Across a distance l from the bottom, v_x rises to values of order u (except near the boundaries between rolls). As noted in Ref. [7], sufficiently close to the bottom and away from the lateral roll boundaries we can approximate the velocity field by a linear profile $v_x=zu/l$, $v_z\sim O(zv_x)$. With this assumption, the boundary layer equation for the temperature at the bottom becomes

$$(uz/l)\,\partial_x T=\partial_z^2 T. \tag{10}$$

The length scale l is determined by the streamfunction distribution only, which is insensitive to changing Ma [cf. Figs. 1(c) and 1(d)]. From Eq. (10), the thickness δ_{bot} of the thermal boundary layer can be estimated either by dimensional analysis or by using the similarity solution in the variable $\xi=z/(lx/u)^{1/3}$ given in Ref. [7]. We find

$$\delta_{bot}\sim u^{-1/3}. \tag{11}$$

Since the heat flux at the top and bottom must be the same, the mean slope of the temperature profile at $z=0$ must be equal to -1. Consequently,

$$\Delta T_{bot}\sim u^{-1/3}. \tag{12}$$

We see that, for large u, the contribution from the bottom boundary layer dominates ΔT. The Nusselt number therefore scales with $u^{1/3}$. Using Eq. (8), we end up with the relation

$$\mathrm{Nu} \sim \mathrm{Ma}^{2/9}. \tag{13}$$

The constant slope of -1 of the mean temperature profile at the top and bottom is obvious from Fig. 2, as well as the increasing difference in thickness between the top and bottom boundary layers. For the scaling of Nu on Ma, the deviation of our numerical exponent 0.24 [cf. Eq. (4)] from the theoretical value of 2/9 is largely due to the contribution of ΔT_{top}. To eliminate this effect, we consider the quantity $\langle T(x,z=0)-T(x,z=1/2)\rangle$ given in Table I, where $\langle\rangle$ denotes the average with respect to x. This quantity is a good measure of ΔT_{bot} for sufficiently large Ma. The theoretical scaling exponent for ΔT_{bot} on Ma is $-2/9$. A power-law fit of the simulation data gives -0.228, which is considerably closer to the theoretical value than the exponent for Nu.

IV. DISCUSSION AND CONCLUSIONS

A prerequisite for the applicability of the $P=\infty$ results for finite P is that the Reynolds number u/P, i.e., the velocity in viscous units, remains small compared with unity. Otherwise, the convective term in Eq. (1a) will affect the streamline pattern, and, together with the time derivative, will eventually cause hydrodynamic instabilities. If we assume that steady laminar convection breaks down at a Reynolds number Re_i, we can estimate the corresponding threshold Ma_i using Eq. (8). The result is

$$\mathrm{Ma}_i \sim P^{3/2}. \tag{14}$$

In our simulations with $P=100$ this threshold was never exceeded, whereas in a simulation with $P=10$ and $\mathrm{Ma}=1.6\times10^5$ the flow turned out to be time dependent.

Experimental measurements of Nu over a wide range of Ma in Bénard-Marangoni convection at large P have so far not been made. The experiments of Eckert *et al.* [22] reached $\mathrm{Ma}\approx 10\mathrm{Ma}_c$, but for the silicone oil-air systems considerable further progress is unlikely. A more promising candidate for large values of Ma may be SF_6 near its critical point, but the feasibility of such experiments requires further analysis. Concentration-driven Marangoni convection at a high Schmidt number (the analog of P), which is governed by the same basic equations, could also be considered as an option.

In conclusion, we have shown that two-dimensional Bénard-Marangoni convection at large P remains steady up to very large values of Ma. The asymptotic state is characterized by laminar boundary layers, which are of different type at the top and bottom. Velocity and heat transport are controlled by the upper and lower thermal boundary layer, respectively. We find a good agreement between our numerical results and the power laws predicted by a phenomenological model.

[1] E.D. Siggia, Annu. Rev. Fluid Mech. **26**, 137 (1994).
[2] J.J. Niemela, L. Skrbek, K.R. Sreenivasan, and R.J. Donnelly, Nature (London) **404**, 837 (2000).
[3] J.A. Glazier, T. Segawa, A. Naert, and M. Sano, Nature (London) **398**, 307 (1999).
[4] X. Chavanne, F. Chillà, B. Castaing, B. Hébral, B. Chabaud, and J. Chaussy, Phys. Rev. Lett. **79**, 3648 (1997).
[5] S. Cioni, S. Ciliberto, and J. Sommeria, J. Fluid Mech. **335**, 111 (1997).
[6] S. Ashkenazi and V. Steinberg, Phys. Rev. Lett. **83**, 3641 (1999).
[7] B.I. Shraiman and E.D. Siggia, Phys. Rev. A **42**, 3650 (1990).
[8] S. Grossmann and D. Lohse, J. Fluid Mech. **407**, 27 (2000).
[9] E.E. DeLuca, J. Werne, R. Rosner, and F. Cattaneo, Phys. Rev. Lett. **64**, 2370 (1990).
[10] R.M. Kerr, J. Fluid Mech. **310**, 139 (1996).
[11] S.H. Davis, Annu. Rev. Fluid Mech. **19**, 403 (1987).
[12] J. Szekely, *Fluid Flow Phenomena in Metals Processing* (Academic Press, New York, 1979).
[13] D.A. Edwards, H. Brenner, and D. T. Wasan, *Interfacial Transport Processes and Rheology* (Butterworth-Heinemann, Boston, 1991).
[14] A. Pumir and L. Blumenfeld, Phys. Rev. E **54**, R4528 (1996).
[15] J.R.A. Pearson, J. Fluid Mech. **4**, 489 (1958).
[16] T. Boeck and A. Thess, J. Fluid Mech. **350**, 149 (1997).
[17] M. Bestehorn, Phys. Rev. E **48**(5), 3622 (1993).
[18] A. Thess and S. Orszag, J. Fluid Mech. **283**, 201 (1995).
[19] L.H. Kellogg and C.A. Stewart, Phys. Fluids A **3**, 1374 (1991).
[20] Instability of the upper thermal boundary layer with respect to hydrothermal waves can occur if the corresponding Marangoni number Ma_{top} (characterizing the horizontal temperature gradient at the free surface) exceeds a finite threshold [M.K. Smith and S.H. Davis, J. Fluid Mech. **132**, 119 (1983)]. We estimate Ma_{top} by $\mathrm{Ma}_{top}\sim\gamma\Delta T_{top}\delta_{top}^2/L\rho\nu\kappa$ with $\Delta T_{\mathrm{top}}/L$ corresponding to the horizontal temperature gradient. From the boundary-layer scalings, it then follows that $\mathrm{Ma}_{top}\sim u^{-3/2}$, i.e., the upper boundary layer cannot become unstable.
[21] G.O. Roberts, Geophys. Astrophys. Fluid Dyn. **12**, 235 (1979).
[22] K. Eckert, M. Bestehorn, and A. Thess, J. Fluid Mech. **356**, 155 (1998).